RSC Advances

PAPER

View Article Online
View Journal | View Issue

Cite this: *RSC Adv.*, 2019, **9**, 36517

The fabrication of a Co_3O_4/graphene oxide (GO)/polyacrylonitrile (PAN) nanofiber membrane for the degradation of Orange II by advanced oxidation technology†

Hao Zhang,[abc] Weihua Liu,[c] Feng Tian,[c] Zhongfeng Tang*[bc] and Haitao Lin*[a]

Treating water that has been polluted with chemical dyes is an important task related to water resources. Advanced oxidation processes are highly efficient for the destruction of organic contaminants. In this study, a Co_3O_4/graphene oxide (GO)/polyacrylonitrile (PAN) filter membrane was prepared through hydrothermal synthesis followed by vacuum filtration. The samples were characterised using different methods. The results showed that the Co_3O_4/GO sheets securely entered the voids of the PAN nanofibres. The Co_3O_4/GO/PAN filter membrane demonstrated the effective degradation of the organic dye Orange II, with a degradation rate of 93.5949%. The degradation rate remained at a high level after five cycles. The Co_3O_4/GO/PAN filter membrane has huge potential for application in industrial dye wastewater treatment.

Received 24th August 2019
Accepted 17th October 2019

DOI: 10.1039/c9ra06656j

rsc.li/rsc-advances

1. Introduction

Water is essential to life, and, although it is very abundant on Earth, it is mainly constituted by aquatic resources that are not directly usable by human beings, such as the ocean and glaciers. Less than 3% of Earth's water can be directly utilized by humans. However, printing and dyeing industries as well as other industrial activity produce abundant quantities of organic dyes that are discharged into natural rivers and lakes. These dyes are usually toxic, carcinogenic, and the processes that will remove them from water are usually difficult. Many different methods, such as adsorption,[1,2] flocculation,[3] biological oxidation[4] and advanced oxidation processes (AOPs),[5] have been applied to exclude organic dyes from wastewater for solving this crisis.

Among these methods, there has been increased interest in AOPs in the research and development (R&D) of wastewater treatment technologies. AOPs can be broadly defined as aqueous phase oxidation methods based on the intermediary of highly reactive species, such as (primarily, but not exclusively) hydroxyl radicals, in the mechanisms leading to the destruction of the target pollutant. During the past 30 years, there have been immense R&D involving AOPs, particularly for two reasons, namely (i) the diversity of technologies involved and (ii) the areas of potential application.[5] Although water and wastewater treatment is by far the most common area for R&D, AOPs have also found applications as diverse as groundwater treatment,[6] soil remediation,[7] municipal wastewater sludge conditioning,[8] ultrapure water production,[9] volatile organic compound treatment,[10] and odour control.[11]

The Fenton reagent is a typical system used with AOPs because it results in the generation of highly reactive hydroxyl radicals through the coupling of a transition metal with an oxidant. The fundamental Fenton reaction initially involved the addition of dilute hydrogen peroxide (H_2O_2) to a degassed solution of iron(II).[12] The reaction provides a very powerful oxidizing agent and is used in several industrial applications for the treatment of contaminated wastewater. However, several significant limitations exist that require resolution: the reaction is effective only at pH values close to 3. At a higher pH value of 6, the efficiency of the Fenton reagent is dramatically decreased due to iron speciation and precipitation.[13]

The system of generating sulfate radicals through the transition metal (*e.g.*, cobalt) decomposition of peroxymonosulfate is a modification of the Fenton reagent. Some research shows that sulfate radicals, generated by the conjunction of transition metals with peroxymonosulfate, are even more efficient oxidants than hydroxyl radicals, and experimentation revealed that the reactivity of the sulfate radicals (such as Co/PMS) was sustained at high pH values, where the efficiency of the Fenton reagent is known to be diminished.[14,15] Attributes such as

[a]*College of Biological and Chemical Engineering, Guangxi University of Science and Technology, Liuzhou, Guangxi, China 545006. E-mail: lhthost@163.com*

[b]*State Key Laboratory for Modification of Chemical Fibers and Polymer Materials, Donghua University, Shanghai 201620, China*

[c]*Shanghai Institute of Applied Physics, Chinese Academy of Sciences, Shanghai, China 201800. E-mail: tangzhongfeng@sinap.ac.cn; Fax: +86-21-39194681; Tel: +86-21-39194681*

† Electronic supplementary information (ESI) available. See DOI: 10.1039/c9ra06656j

efficiency, wide applicability, cost-effectiveness, and no need for an extra energy supply (such as UV) are attractive to the water purification industry. However, when transition metals are formulated into nanometal oxide powders to increase their specific surface area and subsequently improve the catalytic efficiency, this causes harm to the natural environment.[16] Therefore, an environmentally friendly solution that has been utilized is their immobilization on the surface of other materials for practical uses without affecting the degradation efficiency.

Herein, graphene oxide (GO) was chosen as the medium used to fix Co nanoparticles to polyacrylonitrile (PAN) electrospun fibres to prepare Co_3O_4/GO/PAN nanofiber membranes. There are many advantages to using graphene oxide (GO), with a one-atom-thick 2D individual sheet structure.[17] Compared with graphene, GO is hydrophilic and can achieve immense interfacial contact with metal oxide nanoparticles because of its various oxygen-containing functional groups, such as hydroxyls, epoxides, carbonyls, and carboxyls.[18] GO also exhibits a high specific surface area. Therefore, aggregation of nanoparticles can be prevented by loading the nanoparticles onto GO, which provides a large specific surface area for composites[19] (there are many studies describing the synergistic catalysis of metal oxides and graphene in S1†). Electrospun polyacrylonitrile (PAN) nanofiber mats exhibit high porosity, stable chemical properties, low density, large specific surface area, good flexibility, and toughness.[20] Polar nitrile groups contained in PAN molecular chains can also interact with the oxygen-containing groups located on GO sheets. Thus, PAN nanofiber mats used as the basic material to prepare Co_3O_4/GO/PAN combine the advantages of PAN and GO.

In this study, Co_3O_4/GO sheets were prepared by loading Co_3O_4 nanoparticles on GO sheets through hydrothermal synthesis. Then, they were deposited onto an electrospun PAN nanofiber mat through vacuum filtration. The obtained Co_3O_4/GO/PAN nanofiber membrane was characterized in detail through scanning electron microscopy (SEM)/Fourier transform infrared (FTIR) spectroscopy/wide angle X-ray diffraction (WAXD), and its catalytic performance was evaluated through Orange II dye degradation. Orange II reagent is generally used as a model substrate for aromatic azo dyes, which are common contaminants found in wastewater because of their wide industrial uses.[21] Orange II is a widely used synthetic azo dye that does not decompose through biological methods and resists light irradiation and chemical oxidation. Additionally, the degradation mechanism was investigated. The developed Co_3O_4/GO/PAN filter membrane exhibited outstanding degradation ability and reusability.

2. Materials and methods

2.1. Materials

Flake graphite (300 mesh, 99.99%) was provided by Shanghai Yi Fan Graphite Co. Ltd., China. PMS, available as a triple salt of sulphate commercially known as Oxone ($2KHSO_5 \cdot KHSO_4 \cdot K_2SO_4$, 4.5–4.9% active oxygen), was purchased from Shanghai Ansin Chemical Co. Ltd. and used as an oxidant. Cobaltous nitrate $Co(NO_3)_2 \cdot 6H_2O$, sulfuric acid (H_2SO_4, 98%), sodium nitrate ($NaNO_3$), potassium permanganate ($KMnO_4$), dimethyl sulfoxide, *N*,*N*-dimethylformamide (DMF), ethanol, and hydrogen peroxide (H_2O_2, 30%) were supplied by Sinopharm Chemical Reagent Co. Ltd. (China). 5,5-Dimethyl-1-pyrroline-*N*-oxide (DMPO) was obtained from Dojindo Molecular Technologies, Co. Inc. (Japan). PAN with a molecular weight of 150 000 was provided by Aldrich Chemical Co.

2.2. Preparation of Co_3O_4/GO/PAN nanofibers

A Hummers' method[22] was used to prepare the GO from purified natural graphite with a mean particle size of 48.0 μm. Then, GO (50.0 mg) was dispersed into 30.0 mL of 1-hexanol and then sonicated for 3.0 h. The suspension was centrifuged to remove the sediment, and the supernatant was extracted for subsequent use. Subsequently, 1.25 mmol $Co(NO_3)_2 \cdot 6H_2O$ with 20.0 mL of 1-hexanol was mixed with the supernatant by magnetic stirring for 12.0 h. The suspension was centrifuged and washed with ethanol several times. Then, it was dried in a vacuum drying oven at 60.0 °C for 24.0 h to completely remove the remaining 1-hexanol solvent and other sundries.

The PAN nanofiber mat was obtained through electrospinning technology. PAN/DMF solution (10.0 wt%) was obtained by dissolving PAN in DMF with stirring at 80.0 °C. Electrospinning was performed at 16 kV voltage and 0.9 mL h^{-1} spinning rate. The distance between the electrode and the collector was maintained at 10.0 cm. PAN nanofiber was deposited on the aluminium foil of a rolling collector as a ground electrode at the speed of 500.0 rpm.

The prepared Co_3O_4/GO sheets were ultrasonically shaken with 400.0 mL deionized (DI) water for 4.0 h, forming the aqueous dispersion of Co_3O_4/GO sheets. The PAN nanofiber mat was cut into a circle and fixed into a vacuum filtration device, where the aqueous dispersion of Co_3O_4/GO fragments was poured. Vacuum filtration was maintained for 6.0 h, and then, the Co_3O_4/GO/PAN filter membrane was fabricated. The Co_3O_4/GO/PAN filter membrane was rinsed with DI water to remove the Co_3O_4/GO sheets that were not immobilized.

2.3. Degradation of Orange II

Degradation experiments were conducted in two 250.0 mL vessels in which Orange II (0.1 mM) and Oxone (1 mM) were added. Commercial Oxone was used to generate PMS, and 614.7 mg L^{-1} (1 mM) of Oxone was required to release 2.0 mM PMS. Co_3O_4/GO sheets (0.1 g) were attached to the PAN nanofiber. Diacritically, the Co_3O_4/GO/PAN filter membrane was added to one vessel, and the same quality of electrospinning PAN nanofiber was added to the other vessel to confirm the catalytic activity of PAN. Then, the vessels were placed in a water bath containing a constant-temperature vibrator controlled at 25 °C throughout the degradation process.

The Co_3O_4/GO/PAN filter membrane was used as a filter paper with a filtration flask to evaluate its usability, as shown in Fig. 1b. Orange II dye solution (50.0 mL) (0.1 mM) flowed through the filter by gravity in each recycle for approximately 30 min. The concentration of Orange II in the filtrate was

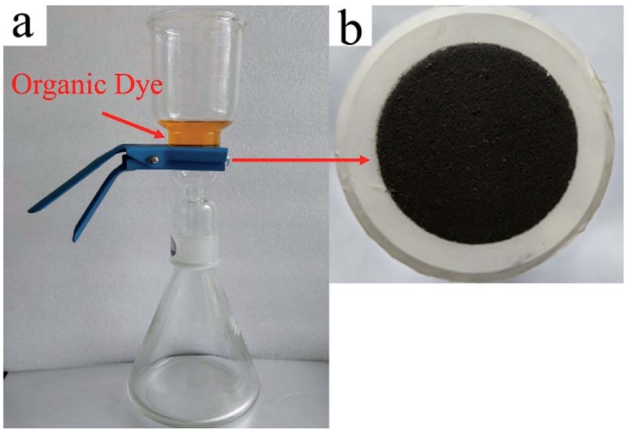

Fig. 1 (a) A photo of the filtration device, and (b) a photo of the fabricated Co_3O_4/GO/PAN filter membrane.

measured by using an ultraviolet-visible (UV-Vis) spectrophotometer (Hitachi U-3900) at 486.0 nm for each run. The Co_3O_4/GO/PAN filter membrane was washed with distilled water and dried at 60 °C in a vacuum after each recycle.

2.4. Characterisation

The chemical bonding information for the Co_3O_4/GO/PAN filter membrane was investigated through FTIR using a potassium bromide (KBr) pellet technique. FTIR spectra were recorded using an Avatar-560 (Nicolet, USA) instrument within the wavenumber range of 600.0–4000.0 cm^{-1}. The atomic composition of the Co_3O_4/GO was detected by X-ray photoelectron spectroscopy (XPS). The XPS spectra were recorded using an Escalab 250Xi photoelectron spectrometer (Thermo Scientific, USA) with Al Kα ($h\nu$ = 1486.6 eV, 500 μm, 150 W) as the X-ray source. The structural features of the Co_3O_4/GO were further confirmed by Raman measurements, whereby the Raman spectroscopy of the samples was recorded using an in *via* Raman microscope (Renishaw, UK). The morphology of the sample was characterised through SEM (JSM-5600LVSEM, JEOL, Japan) at an accelerating voltage of 10 kV.

WAXD was conducted using a 16B Beamline equipped with a Rayonix-2M detector at the Shanghai Synchrotron Radiation Facility. The samples were systematically sandwiched between two pieces of Kapton tape for the preferred orientation effect. The chosen wavelength was 0.124 nm. The distance between sample and the detector was 12.8 cm, and the data were collected for 20 s for all the measurements.

The concentration of Orange II was determined through UV-Vis spectrophotometry using a U-3900 spectrophotometer (Hitachi, Japan). The concentration of Orange II was measured on the basis of the Beer–Lambert law:[23]

$$A = abc$$

where a denotes the absorption coefficient (L g^{-1} cm^{-1}), b denotes the distance travelled by the light in the sample (cm), and c denotes the concentration of the solution (g L^{-1}). A linear relationship between the absorbance and concentration of the solution was assumed. The degradation rate (D%) was calculated.

$$D(\%) = \frac{A_0 - A_i}{A_0} \times 100$$

where A_0 is the absorbance of the original organic dye solution, and A_i denotes the absorbance of the i(th) time for the recycling degradation experiments. The radicals formed in Oxone were investigated based on electron spin resonance (ESR) spectra obtained from a JES-FA 200 (JEOL, Japan) electron spin resonance spectrometer with DMPO as the spin-trapping agent.

3. Results and discussion

3.1. Characterisation of the Co_3O_4/GO/PAN filter membrane

Co_3O_4/GO sheets were obtained through hydrothermal synthesis and were fixed onto the PAN nanofiber mat through vacuum filtration. The FTIR spectra were used to characterise the chemical structure of the Co_3O_4/GO sheets and the Co_3O_4/GO/PAN membrane, as shown in Fig. 2. The peaks at 1449.0 and 2928.0 cm^{-1} in the IR spectrum for the PAN electrospun nanofiber (curve a) were assigned to the bending and stretching vibrations of C–H, respectively. The peak at 2246 cm^{-1} was attributed to the stretching vibration of –C≡N, which is the characteristic peak of PAN.[24] In the IR spectrum for Co_3O_4/GO (curve b), the peaks at 3405 and 1208 cm^{-1} were attributed to the O–H stretching and bending vibrations of GO, respectively. The stretching vibration of C=O in carboxylic acid or carbonyl moieties[25–28] was responsible for the peak at 1722 cm^{-1}, and the skeletal vibration of GO sheets[29,30] was responsible for the peak at 1580 cm^{-1}.

The IR spectrum for Co_3O_4/GO showed a strong peak at 663 cm^{-1} because of the formation of Co_3O_4 spinel oxide,[31] confirming the existence of Co_3O_4. Apparently, all the characteristic peaks from PAN, GO, and Co_3O_4 were observed in the IR

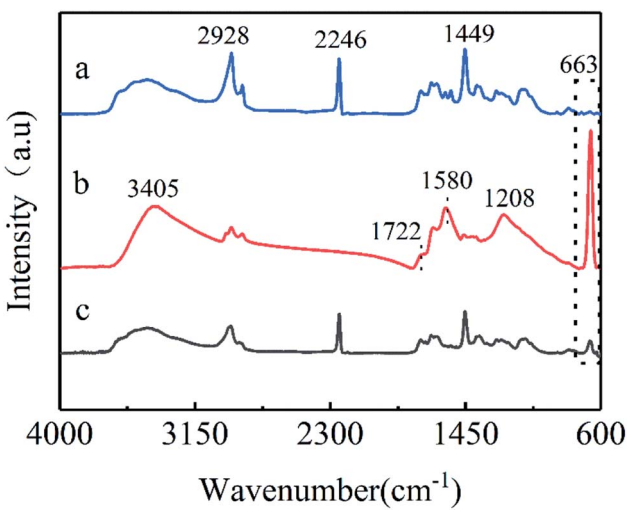

Fig. 2 FTIR spectra of (a) electrospun PAN nanofibers, (b) Co_3O_4/GO, and (c) the Co_3O_4/GO/PAN filter membrane.

spectrum for the Co_3O_4/GO/PAN filter membrane (curve c), indicating that the Co_3O_4/GO sheets were successfully attached to the PAN nanofiber. No new peaks were observed in the IR spectrum for Co_3O_4/GO/PAN. Co_3O_4/GO was loaded on the PAN nanofibers, but not through chemical bonds.

The chemical state of the elements in Co_3O_4/GO is provided by XPS measurement. The binding energies of samples obtained *via* XPS analyses were corrected for specimen charging by referencing the C 1s peak to 284.7 eV. Fig. 3a shows the C 1s, O 1s, and Co 2p peaks for Co_3O_4/GO. The Co 2p XPS spectra illustrated in Fig. 3b show two major peaks with binding energies at 780.5 eV and 786.1 eV, assigned to Co $2p_{3/2}$ and Co $2p_{1/2}$, respectively.

Two shake-up satellite peaks located around the main peaks at approximately 803.9 eV and 787.7 eV are characteristic of a Co_3O_4 phase I.[29,32,33] The C 1s peak shown in Fig. 3c clearly indicates a considerable degree of oxidation, with three components that correspond to carbon atoms in different functional groups: the carbon in C–C, C=C, and C–H at 284.7 eV.; the carbon in C–O at 286.3 eV; and the carbonyl carbon (C=O) at 288.3 eV,[34] respectively. This proves that carbon in the form of GO exists in the sample. Raman I_D/I_G ratios (where I_D and I_G are the D-band and G-band Raman intensities, respectively) are widely used to evaluate the quality of carbon materials. As shown in Fig. 3d, the relative intensity (I_D/I_G) ratio of the D (1345 cm^{-1}) and G bands (1598 cm^{-1}) for Co_3O_4/GO is 1.09, close to the graphene nanoribbons (1.0–1.5) synthesized,[35] and it is also highly consistent with the reports in the literature.[34]

SR-WAXD is usually used to investigate the crystalline properties of materials. Fit2D (v12.077) software was used to process SR-WAXD patterns. 2D WAXD results for PAN nanofibers were obtained. The Co_3O_4/GO/PAN filter membrane is shown in Fig. 4a and b, and the integrated 1D WAXD patterns are shown in Fig. 4c. For PAN, a broad diffraction peak at $2\theta = 28.26^\circ$ was observed, which corresponded to the pristine graphite[27] for Co_3O_4/GO/PAN. No new peak was observed, indicating that no new crystal structure was formed between PAN and GO in the Co_3O_4/GO/PAN membrane. Combined with the FTIR analysis, this indicated that the loading of the Co_3O_4/GO sheets on the PAN nanofibers occurred *via* physical interaction.

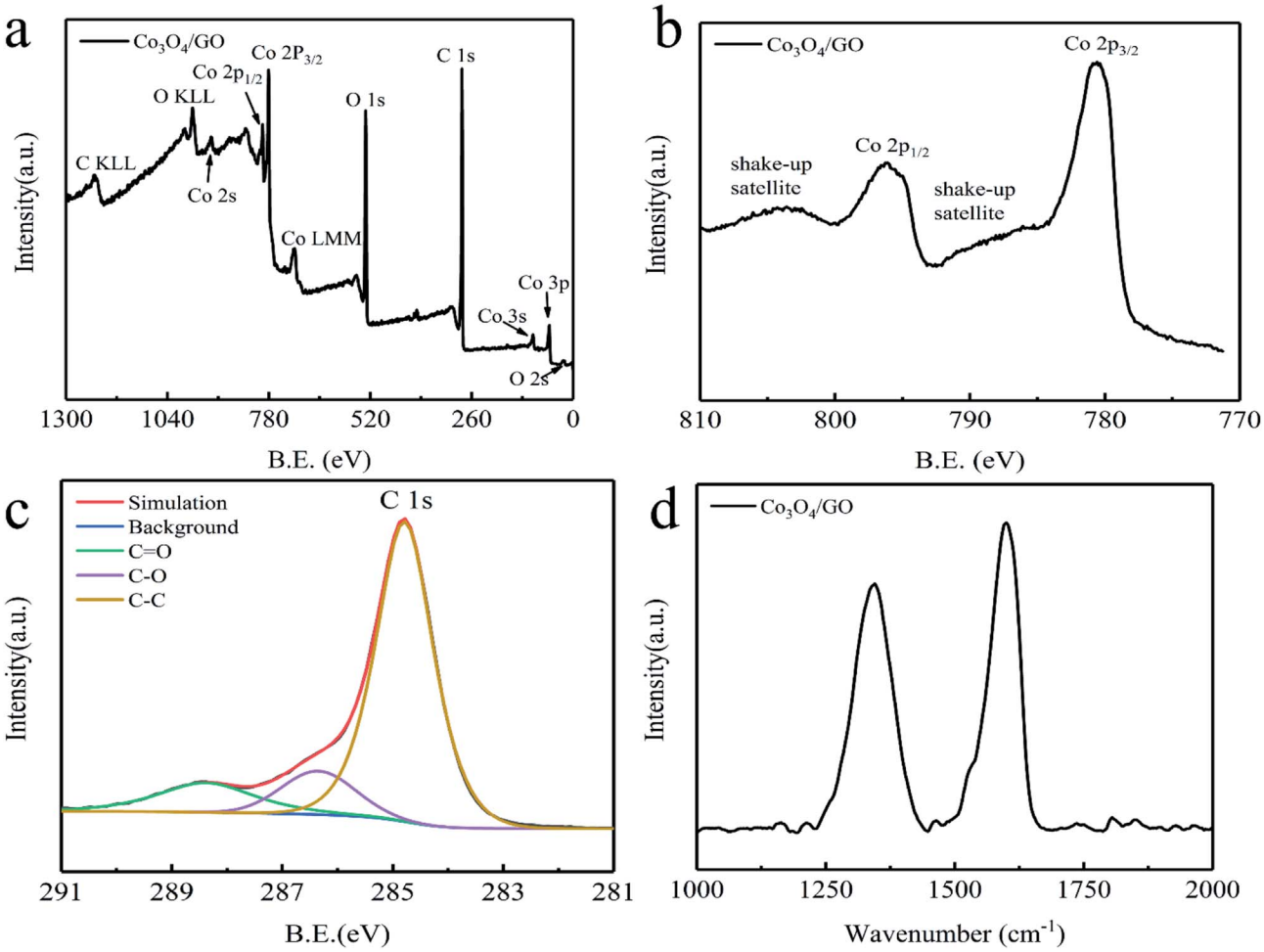

Fig. 3 (a) XPS survey spectrum for Co_3O_4/GO, (b) the Co 2p XPS spectrum for Co_3O_4/GO, (c) the C 1s XPS spectrum for GO and Co_3O_4/GO, and (d) the Raman spectrum for Co_3O_4.

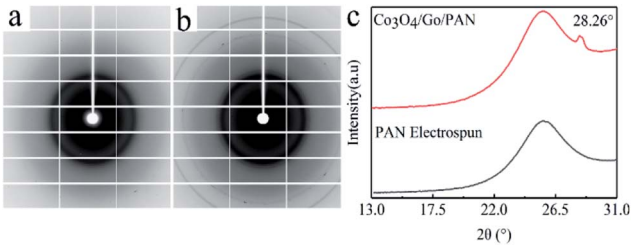

Fig. 4 2D-WAXD patterns of (a) electrospun PAN nanofibers, and (b) the Co_3O_4/GO/PAN filter membrane; (c) the WAXD spectra of 1D-WAXD, processed by FIT2D.

Typical SEM images of PAN nanofibers, Co_3O_4/GO, and the Co_3O_4/GO/PAN filter membrane are shown in Fig. 5. PAN nanofibers had a diameter of approximately 300 nm and exhibited high permeability and porosity. Co_3O_4 particles were dispersed on the surface of the GO without obvious aggregation (Fig. 5c). Co_3O_4/GO sheets were entrapped inside the 3D network formed by the PAN nanofibers. The EDS spectra of the Co_3O_4/GO/PAN filter membrane (Fig. 6) confirmed the presence of cobalt and carbon, indicating that Co_3O_4 particles were successfully loaded onto the PAN nanofibre mat.

Fig. 6d shows the chemical composition of the tested samples. The content of carbon was 89%, which was higher than that of pure PAN (at approximately 68%). GO contributed to the high carbon content, signifying that the Co_3O_4/GO sheets were securely combined with PAN to enter the void of the PAN nanofibers. The results were consistent with those of FTIR and also the SEM morphology.

3.2. Catalytic performance of the Co_3O_4/GO/PAN membrane

A pure PAN nanofiber mat and Co_3O_4/GO/PAN were used to catalyse the degradation of Orange II under the same conditions to investigate the degree of degradation that was obtained. As indicated in the experimental section, degradation experiments were conducted in two 250.0 mL-beakers, both containing Orange II (0.1 mM) and Oxone (1.0 mM).

After 1 h degradation, no changes were observed in the Orange II dye solution that was in the presence of the PAN nanofiber mat. At the same time, the solution in the presence of the Co_3O_4/GO/PAN membrane essentially became colourless, as shown in Fig. 7a. This condition indicated that the PAN nanofiber did not contribute to the degradation of Orange II in the presence of Oxone. The Co_3O_4/GO/PAN membrane exhibited good catalytic activity for the degradation of Orange II. Hence,

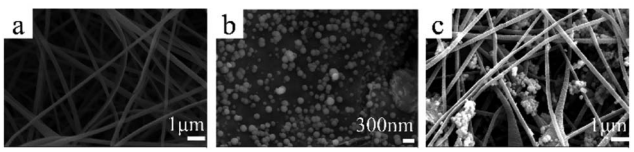

Fig. 5 SEM images of (a) PAN nanofibers, (b) Co_3O_4/GO/PAN nanofibers, and (c) Co_3O_4/GO.

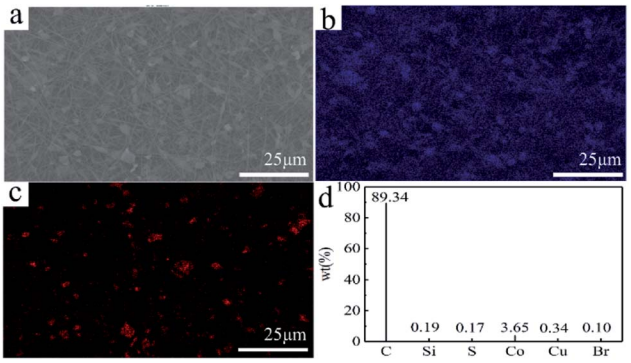

Fig. 6 An SEM image of (a) the Co_3O_4/GO/PAN filter membrane, the SEM-EDS mapping of (b) C elements and (c) Co elements, and (d) the corresponding chemical compositions.

Co_3O_4/GO sheets degraded Orange II in water by advanced oxidation technology based on sulphate radicals.

Five recycling runs were performed to investigate the reusability of the Co_3O_4/GO/PAN membrane during practical applications. In the recycling experiments, Co_3O_4/GO/PAN or the PAN mat was used as the filter membrane in a setup with a filtration flask (Fig. 1), and 50.0 mL Orange II solution flowed through the membrane by gravity. Each run took approximately 30.0 min. The solution became colourless when the cycle completed.

The degradation rates for five runs are presented in Fig. 7b. The degradation rate was more than 90.0% for the first run, although the retention time was short for the solution, indicating the high catalytic activity of Co_3O_4/GO/PAN. The activity of the membrane slightly decreased compared with the fresh catalyst, which may be related to the loss of catalyst during washing and drying after each run. (The result of spectroscopic characterization of the membrane before and after degradation is shown in S2†). For pure PAN, no catalytic effect upon degradation nor absorption effect of Orange II was observed. PAN was used as the loading material to facilitate the recycling of the catalyst because of its high toughness and chemical stability.

Compared with common catalysts of metal oxide materials (such as Fe ions[36]), the Co_3O_4/GO/PAN filter membrane showed

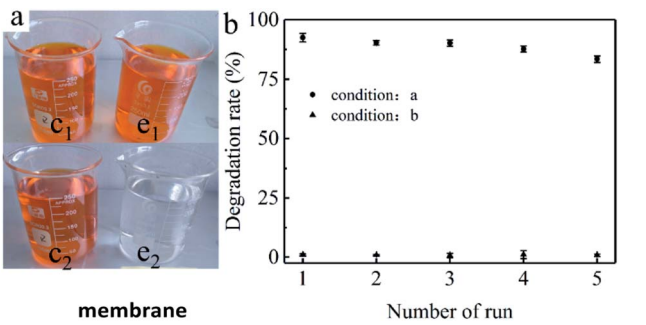

Fig. 7 (a) Photos showing the catalytic activities of PAN (c_1, c_2) and Co_3O_4/GO/PAN (e_1, e_2); c_1 and e_1 are the original dye solutions with PAN and Co_3O_4/GO/PAN, respectively; c_2 and e_2 are the corresponding dye solutions one hour later of c_1 and e_1, respectively. (b) The degradation rate of the filter device with the Co_3O_4/GO/PAN filter membrane (●) and PAN nanofiber mat (▲).

a high degradation rate and good reusability. The dye degradation process did not require an extra light source, rendering it suitable for many applications.

3.3. Catalytic mechanism of the Co_3O_4/GO/PAN filter membrane

Fig. 8 illustrates the fabrication of the Co_3O_4/GO/PAN filter membrane and its working mechanism. First, Co_3O_4/GO sheets were synthesised *via* a hydrothermal synthesis. Then, the Co_3O_4/GO sheets were attached to the PAN fibres through vacuum filtration. Finally, PMS was activated by Co^{2+} ions to become $SO_4^{-\bullet}$ and ·OH free radicals during the degradation of Orange II when the organic dye flowed through the Co_3O_4/GO/PAN filter membrane in the presence of PMS.

As shown in Fig. 9, seven-line spectra were observed, which were primarily assigned to the DMPO-SO_4 formed by the addition of DMPO to $SO_4^{-\bullet}$.[37,38] $SO_4^{-\bullet}$ radicals were formed within 3 min, and the concentration of [$SO_4^{-\bullet}$] radicals initially increased and then gradually decreased. The peak of the ESR spectrum slightly deviated from the data in the reported literature.[39] This condition may be caused by the combination of signals from the addition product of DMPO to ·OH. Combined with the above characterization information, several reactions occurred during the degradation of Orange II, which are described as follows:[15,29,40]

$$Co^{2+} + HSO_5^- \rightarrow Co^{3+} + SO_4^{-\bullet} + OH^-$$

$$Co^{3+} + HSO_5^- \rightarrow Co^{2+} + SO_5^{-\bullet} + H^+$$

$$SO_4^{-\bullet} + H_2O \rightarrow SO_4^{2-} + \cdot OH + H^+$$

$$SO_4^{-\bullet} + \text{organic dyes [Orange II]} \rightarrow \text{intermediate products} \rightarrow CO_2 + H_2O$$

$$\cdot OH + \text{organic dyes [Orange II]} \rightarrow \text{intermediate products} \rightarrow CO_2 + H_2O$$

The catalytic effect of the Co_3O_4/GO/PAN filter membrane was validated. The formed radicals were detected through ESR by using DMPO as a radical spin-trapping agent. DMPO (3 μL) was added to 3 mL organic dye (Orange II) with 1 mM PMS and 0.1 g L^{-1} Co_3O_4/GO sheets.

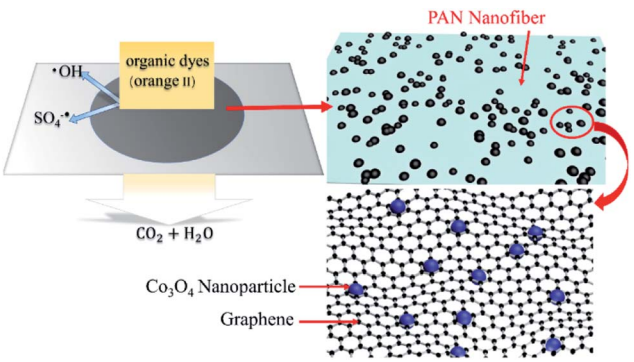

Fig. 8 A schematic diagram of the fabrication process and the proper working mechanism of Co_3O_4/GO/PAN.

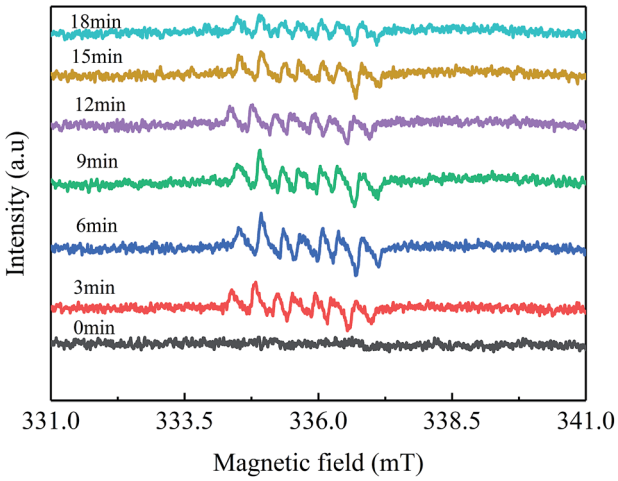

Fig. 9 ESR spectra of Co_3O_4/GO as a catalyst in the presence of PMS at room temperature at different times.

4. Conclusions

Graphene oxide (GO) was used as a medium to fix Co nanoparticles onto PAN electrospun fibers to prepare a Co_3O_4/GO/PAN nanofiber membrane. Samples of this material were characterised *via* different methods. The results showed that the Co_3O_4/GO sheets securely entered the voids of the PAN nanofibers. No chemical bonds formed between the Co_3O_4/GO fragments and the PAN nanofibers, which indicated that the Co_3O_4/GO fragments and other catalysts can be fixed onto PAN nanofibers.

Degradation experiments showed that the filter membrane can effectively degrade organic dyes, such as Orange II, with a degradation rate of 93.5949%. The degradation rate remained at a high level after five cycles. The Co_3O_4/GO/PAN filter membrane showed high catalytic activity for the degradation of Orange II in water through advanced oxidation technology based on sulphate radicals. The Co_3O_4/GO/PAN filter membrane has great potential for application in industrial dye wastewater treatment.

Conflicts of interest

There are no conflicts to declare.

Acknowledgements

This project was founded by the State Key Laboratory for the Modification of Chemical Fibers and Polymer Materials, Donghua University (KF1813). The project is supported by the Science and Technology Commission of Shanghai Municipality (grant no. 11JC1414900).

References

1 G. Crini and P. M. Badot, *Prog. Polym. Sci.*, 2008, **33**, 399–447.
2 X. Yuan, S. P. Zhuo, W. Xing, H. Y. Cui, X. D. Dai, X. M. Liu and Z. F. Yan, *J. Colloid Interface Sci.*, 2007, **310**, 83–89.
3 E. Guibal and J. Roussy, *React. Funct. Polym.*, 2007, **67**, 33–42.
4 I. Oller, S. Malato and J. A. Sánchez-Pérez, *Sci. Total Environ.*, 2011, **409**, 4141–4166.
5 C. Comninellis, K. Agnieszka, M. Sixto, S. A. Parsons, P. Ioannis and M. Dionissios, *J. Chem. Technol. Biotechnol.*, 2008, **83**, 769–776.
6 Y. Zhou, Y. Xiang, Y. He, Y. Yang, J. Zhang, L. Luo, H. Peng, C. Dai, F. Zhu and L. Tang, *J. Hazard. Mater.*, 2018, **359**, 396–407.
7 M. Cheng, G. Zeng, D. Huang, C. Lai, P. Xu, C. Zhang and Y. Liu, *Chem. Eng. J.*, 2016, **284**, 582–598.
8 K. V. Lo, H. Tan, I. Tunile, T. Burton, T. Kang, A. Srinivasan and P. H. Liao, *Chem. Eng. Process.*, 2018, **128**, 143–148.
9 D. Bhaumik, S. Majumdar, Q. Fan and K. K. Sirkar, *J. Membr. Sci.*, 2004, **235**, 31–41.
10 F. A. Almomani, R. R. Bhosale, A. Kumar and C. Kennes, *Sol. Energy*, 2016, **135**, 348–358.
11 D. Wang, J. R. Bolton, S. A. Andrews and R. Hofmann, *Chemosphere*, 2015, **136**, 239–244.
12 F. J. Rivas, F. J. Beltrán, O. Gimeno and J. Frades, *J. Agric. Food Chem.*, 2001, **49**, 1873–1880.
13 F. J. Rivas, F. J. Beltrán, J. Frades and P. Buxeda, *Water Res.*, 2001, **35**, 387–396.
14 G. P. Anipsitakis and D. D. Dionysiou, *Environ. Sci. Technol.*, 2003, **37**, 4790–4797.
15 G. P. Anipsitakis and D. D. Dionysiou, *Environ. Sci. Technol.*, 2004, **38**, 3705–3712.
16 G. Oberdörster, V. Stone and K. Donaldson, *Nanotoxicology*, 2007, **1**, 2–25.
17 A. K. Geim and K. S. Novoselov, *Nat. Mater.*, 2007, **6**, 183.
18 R. Li, C. Liu and J. Ma, *Carbohydr. Polym.*, 2011, **84**, 631–637.
19 K. Sun, L. Wang, C. Wu, J. Deng and K. Pan, *Adv. Mater. Interfaces*, 2017, 1700845.
20 J. Wang, P. Zhang, B. Liang, Y. Liu, T. Xu, L. Wang, B. Cao and K. Pan, *ACS Appl. Mater. Interfaces*, 2016, **8**, 6211–6218.
21 G. Crini, *Prog. Polym. Sci.*, 2005, **30**, 38–70.
22 D. C. Marcano, D. V. Kosynkin, J. M. Berlin, A. Sinitskii, Z. Sun, A. S. Slesarev, L. B. Alemany, W. Lu and J. M. Tour, *ACS Nano*, 2018, **12**, 2078.
23 K. Fuwa and B. L. Vallee, *Anal. Chem.*, 1963, **35**, 942–946.
24 D. Zhang, A. B. Karki, D. Rutman, D. P. Young, A. Wang, D. Cocke, T. H. Ho and Z. Guo, *Polymer*, 2009, **50**, 4189–4198.
25 Y. Xu, H. Bai, G. Lu, C. Li and G. Shi, *J. Am. Chem. Soc.*, 2008, **130**, 5856–5857.
26 Y. Xu, Z. Liu, X. Zhang, Y. Wang, J. Tian, Y. Huang, Y. Ma, X. Zhang and Y. Chen, *Adv. Mater.*, 2009, 1275–1279.
27 H. Guo, X. Wang, Q. Qian, F. Wang and X. Xia, *ACS Nano*, 2009, **3**, 2653–2659.
28 Y. Si and E. T. Samulski, *Nano Lett.*, 2008, **8**, 1679–1682.
29 P. Shi, R. Su, F. Wan, M. Zhu, D. Li and S. Xu, *Appl. Catal., B*, 2012, **123–124**, 265–272.
30 H. W. Wang, Z. A. Hu, Y. Q. Chang, Y. L. Chen, Z. Y. Zhang, Y. Y. Yang and H. Y. Wu, *Mater. Chem. Phys.*, 2011, **130**, 672–679.
31 R. Xu and H. C. Zeng, *Langmuir*, 2004, 9780–9790.
32 Z. Y. Wu, P. Chen, Q. S. Wu, L. F. Yang, Z. Pan and Q. Wang, *Nano Energy*, 2014, **8**, 118–125.
33 S. Schmid, R. Hausbrand and W. Jaegermann, *Thin Solid Films*, 2014, **567**, 8–13.
34 S. Stankovich, D. A. Dikin, R. D. Piner, K. A. Kohlhaas, A. Kleinhammes, Y. Jia, Y. Wu, S. B. T. Nguyen and R. S. Ruoff, *Carbon*, 2007, **45**, 1558–1565.
35 P. Pachfule, D. Shinde, M. Majumder and Q. Xu, *Nat. Chem.*, 2016, **8**, 718–724.
36 I. Sirés, J. A. Garrido, R. M. Rodríguez, E. Brillas, N. Oturan and M. A. Oturan, *Appl. Catal., B*, 2007, **72**, 382–394.
37 C. Tan, N. Gao, Y. Deng, J. Deng, S. Zhou, J. Li and X. Xin, *J. Hazard. Mater.*, 2014, **276**, 452–460.
38 Y. Wang, X. Zhao, D. Cao, Y. Wang and Y. Zhu, *Appl. Catal., B*, 2017, **211**, 79–88.
39 G. D. Fang, D. D. Dionysiou, S. R. Al-Abed and D. M. Zhou, *Appl. Catal., B*, 2013, **129**, 325–332.
40 W. Zhang, H. L. Tay, S. S. Lim, Y. Wang, Z. Zhong and R. Xu, *Appl. Catal., B*, 2010, **95**, 93–99.